Velocity Inversion with an Iterative Normal Incidence Point (NIP) Wave Tomography with Model-Based Common Diffraction Surface (CDS) Stack

Hashem Shahsavani [1*] and Fatemeh Pourkamar [2]

[1] *Assistant Professor, Department of Mining-Faculty of Engineering-University of Kurdistan-Sanandaj-Iran*

[2] *Msc Student, Department of Mining-Faculty of Engineering-University of Kurdistan-Sanandaj-Iran*

(Received: 10 July 2019, Accepted: 16 October 2019)

Abstract

Normal Incidence Point (NIP) wave tomography inversion has been recently developed to generate a velocity model using Common Reflection Surface (CRS) attributes, which is called the kinematic wavefield attribute. In this paper, we propose to use the model based Common Diffraction Surface (CDS) stack method attributes instead of data driven Common Reflection Surface attributes as an input data parameter. In this way, the effects of Normal wave on Normal Incidence Point wave calculation are removed. In the proposed method, the velocity model is updated iteratively by an interactive between Common Diffraction Surface attributes and the velocity model produced by Normal Incidence Point wave tomography inversion. We applied the proposed method on a 2D complex land data set in the northeast of Iran. The events in the Common Image Gathers (CIGs) become flat after migrating the pre stack data by using the obtained velocity. This is while the events on the same Common Image Gathers that are processed by the data driven Common Reflection Surface stake method are not well flatted. These results show a great capability of the proposed method to obtain the velocity model compared to the single step Normal Incidence Point wave tomography inversion with Common Reflection Surface attributes.

Keywords: Inversion, Tomography, CRS, CDS

*Corresponding author: h.shahsavani@uok.ac.ir

1 Introduction

The CRS stack method, which is a generalized form of Common-Mid-point (CMP) method, not only simulates the Zero-Offset (ZO) stack section with high Signal to Noise Ratio (SNR) but also generates very useful attributes as byproducts. One of the methods that use these attributes is NIP wave tomography inversion. In this method, a smooth velocity model is obtained by iteratively minimizing the difference between a model parameter and data parameter generated by the CRS stack method; i.e. R_{NIP} and alpha (Duveneck, 2004). The CRS stack method in its basic form (Jäger, 1999; Mann et al., 1999; Müller et al., 1998) is unable to handle the conflicting dips. Later on, this problem was addressed and solved to some extent (Mann, 2002). By merging the concept of Dip-Move-Out (DMO) and CRS stack method, the CDS stack method was introduced (Soleimani et al., 2009a). This method addresses the conflicting dip into the full extent (Soleimani et al., 2009b).

By applying the CRS operator on certain common offset (CO), the partial CRS stack has been introduced (Baykulov and Gajewski, 2009). This idea has been applied to CDS stack operator successfully (Soleimani and Rafiei, 2016). The partial CRS has been implemented on a land data set in Iran with impressive results (Pahlavanloo et al., 2017).

The CDS attributes are calculated by applying coherence analysis on the pre-stack multi-coverage data set, which is computationally very expensive. By performing the concept of kinematic and dynamic ray tracing on a smooth velocity model with a lower accuracy, the CDS attributes are obtained in an efficient and fast manner (Shahsavani et al., 2011). The attribute R_{NIP}, which is produced by CRS stack method by coherence analysis in a data-driven manner is affected by R_N, while $R_{CDS} \equiv R_{NIP}$ is obtained by the CDS independent of R_N. Therefore, it is more accurate (Shahsavani, 2011). In this work, we propose using R_{CDS} instead of R_{NIP} obtained from the CRS stack method. The CDS method is first applied to the constant velocity model, and then NIP tomography inversion is applied with respect to obtained attributes to achieve a new velocity model. Again, the CDS method is performed on the new velocity model and the new attributes are generated. This process iteratively is repeated until the velocity model does not change significantly.

2 Theory

Hubral (1983) introduced two hypothetical experiments (Hubral, 1983). One of these experiments is related to an exploding diffractor that produces NIP wave with radius R_{NIP} at the surface. Another experiment is related to an exploding reflector and generates the normal (N) wave with radius R_N at the surface. Both radii are defined at the emergence location of the normal ray. Figure 1 is illustrated these waves and their emergence angel. R_{NIP}, R_N, and the emergence angle are called kinematic wavefield attributes.

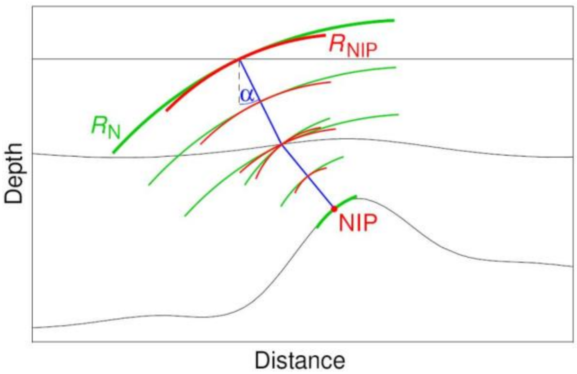

Figure 1: Two hypothetical experiment generates two hypothetical waves, NIP wave and Normal (N) wave, the emergence angle of these two waves at the surface is equal (Hertweck et al., 2007)

Based on two hypothetical wavefronts and their emergence angle (i.e., Kinematic wavefield attributes), the CRS stack travel time is obtained using different concepts (Höcht et al., 1999; Schleicher et al., 1993; Tygel et al., 1997) as follows:

$$t^2(x_m, h) = \left[t_0 + \frac{2sin\alpha}{v_0}(x_m - x_0)\right]^2 + \frac{2t_0\, cos^2\alpha}{v_0}\left[\frac{(x_m - x_0)^2}{R_N} + \frac{h^2}{R_{NIP}}\right], \quad (1)$$

where t is the travel time of the reflection, v_0 the near-surface velocity, h the half offset, x_0 and t_0 are the location and travel time of the selected ZO output sample (x_0, t_0), respectively, x_m is the distance of the midpoint between the shot (S) and receiver location (R) from x_0, R_N is the radius of the hypothetical normal (N) wave, R_{NIP} is the radius of the hypothetical NIP-wave, and α is their common emergence angle.

For a diffractor at the depth, R_{NIP} is equal to R_N so-called R_{CDS}. Therefore, Eq. (1) is simplified to:

$$t^2(x_m, h) = \left[t_0 + \frac{2sin\alpha}{v_0}(x_m - x_0)\right]^2 + \frac{2t_0\, cos^2\alpha}{v_0 R_{CDS}}[(x_m - x_0)^2 + h^2], \quad (2)$$

This equation can image the diffraction into full extent. However, for the reflector, a reasonable aperture is needed because for each angle, the desired R_{CDS} is obtained by coherence analysis in pre-stack data, which is a very time-consuming process. Hence, it is proposed to use ray tracing to obtain RCDS for each emergence angle on a smooth velocity model. For this purpose, the kinematic and dynamic equations have to be solved simultaneously.

The NIP tomography inversion uses some pick points from the sections that are produced using the CRS stack method as data parameters:

$$(\mathrm{T}, \mathrm{M_h}, \mathrm{p_\xi}, \xi)_\mathrm{i}, \mathrm{i} = 1, 2, 3, \ldots, \mathrm{ndata} \quad (3)$$

where T is one way travel time ($T=t_0/2$), M_h relates to NIP wave curvature, p_ξ is the slowness vector at surface location ξ, and ξ is the location at the surface.

The model parameter is defined as follows:

$$(\mathrm{x}, \mathrm{z}, \mathrm{p_x})_\mathrm{i} \quad \mathrm{i} = 1, 2, 3, \ldots, \mathrm{ndata} \qquad \mathrm{v_{jk}}\ \mathrm{j} = 1,2,3, \ldots, \mathrm{n_{data}}, \quad \mathrm{k} = 1,2,3, \ldots, \mathrm{n_{data}} \quad (4)$$

The velocity model has nx horizontal and nz vertical grid points.

A model vector **m**, consisting of the elements given in Eq. (4), is found in a way that minimizes the misfit between a data vector **d** and the model values.

It is possible to write the inversion equation as:

$$\mathbf{d_{mod}} = \mathbf{f}(\mathbf{m}), \quad (5)$$

where **f** is a function of **m**. Hence, Eq. (5) is nonlinear and has to be solved iteratively. The details of the strategy to solve Eq. (5) are explained in (Duveneck and Hubral, 2002).

3 Implementation

The model-based CDS stack method needs a smooth velocity model and produces the attributes needed for NIP tomography (i.e. $R_{CDS} \equiv R_{NIP}$ and α). Consequently, it is possible to calculate a new smooth velocity model based on these attributes by NIP wave tomography inversion. Then, the new attribute can be produced by applying the CDS stack method on this refined smooth velocity model. This process is repeated until the variation of the velocity model is not significant. A simplified flow chart of the proposed method is shown in Figure 2.

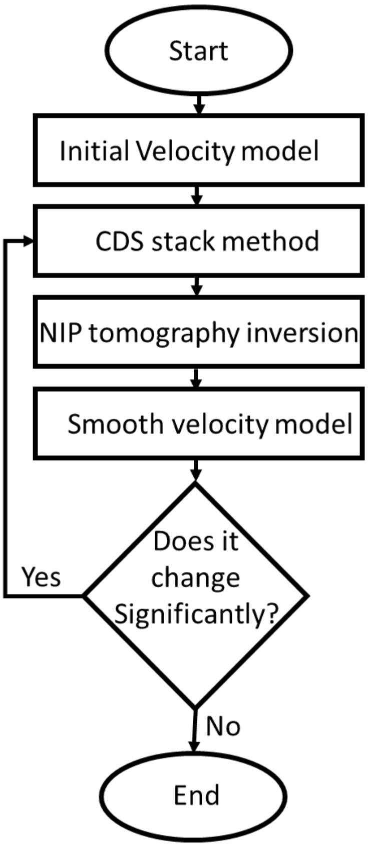

Figure 2: A simplified flow chart of the proposed method.

Table 1. Data acquisition parameters.

Title	Amount
Shot Interval	70 m
Group Interval	35 m
Number of Shots	479
Number of Active Channels	96
Number of CMPs	1948
CMP Distance	18 m
Sampling Interval	0.004sec
Number of Sample per Trace	1875

Real data example

The proposed method was applied to real land data for the northwest of Iran. The geometrical acquisition parameters are listed in Table 1.

The model-based CDS stack method is initially applied on a constant velocity model V_{const}=3000 m/s, and the attribute sections are obtained. These attributes sections are shown for the first round in Figure 3.

The attribute illustrated in Figure 3 is used for NIP wave tomography inversion. The smooth velocity model obtained in each round is shown in Figure 4.

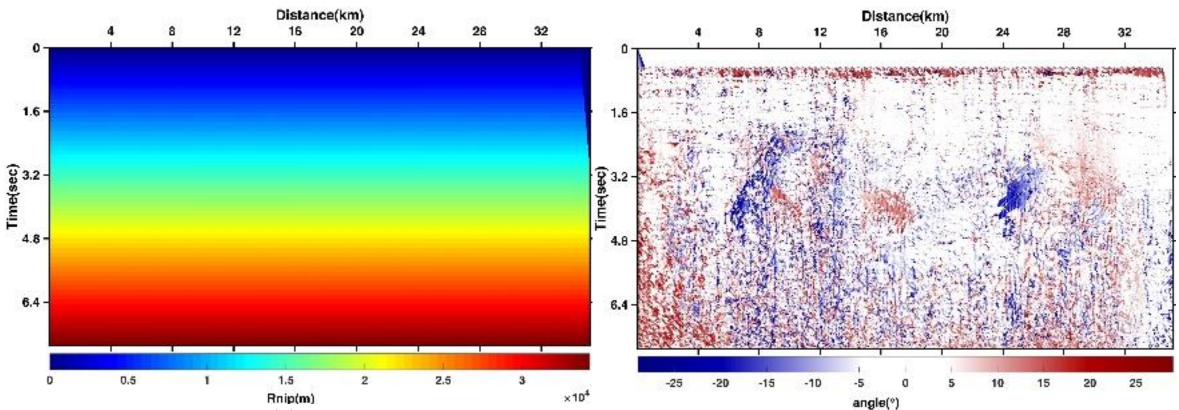

(a) (b)

Figure 3: Attributes of the CDS stack method in the first round a) section of R_{CDS} radius, and b) the emergence angle.

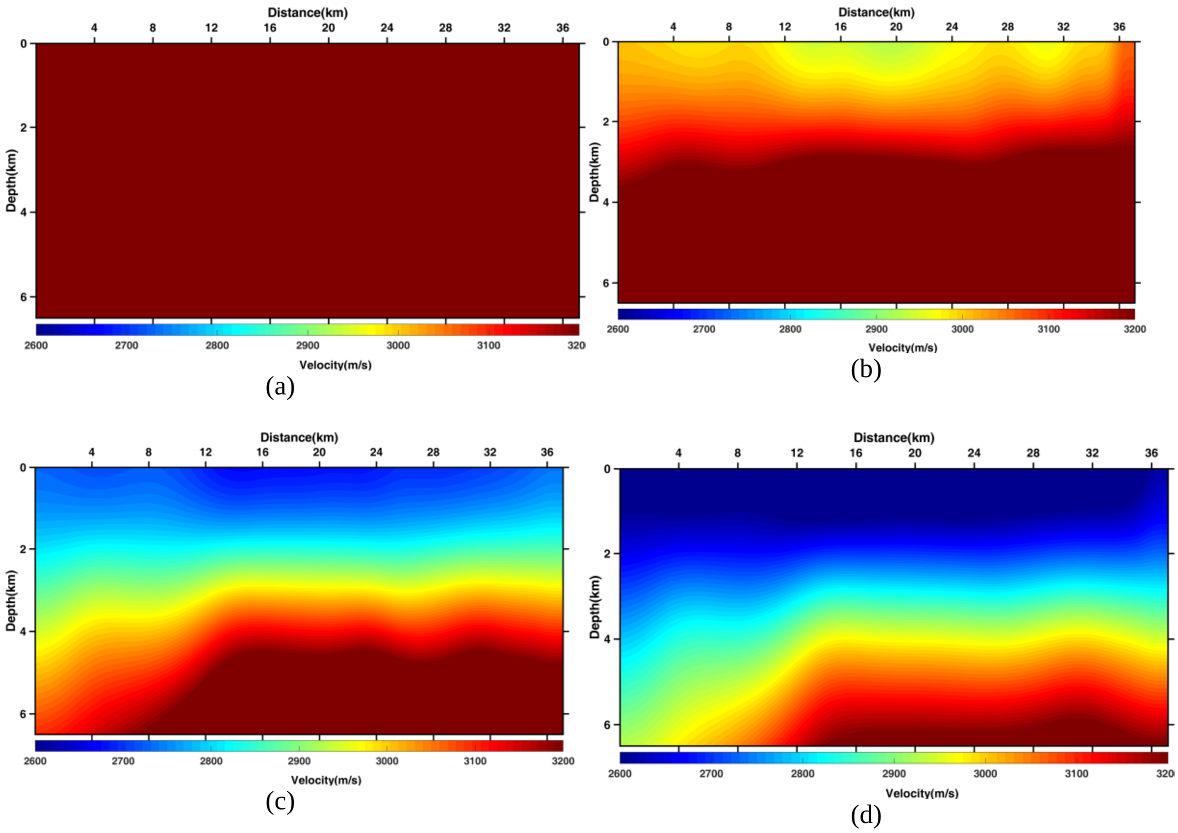

Figure 4: The smooth velocity model calculated in each round from 'a' to 'd', round two to five respectively.

The smooth velocity model in Figure 4a is applied by the CDS stack method to produce wavefield attributes. Next, the attributes (not shown here) are used by NIP tomography to generate the smooth velocity model shown in Figure 4b. Analogously, the smooth velocity models are calculated (Figure 4c to Figure 4e).

In addition to wave filed attributes, the CDS stack method generates the coherence section. In the proposed method, in each round, the coherence increased, suggesting the improvement of the velocity model. These coherence sections are depicted in Figure 5.

The CRS stack method was applied to the data. Then, the smooth velocity model shown in Figure 6 was obtained by NIP tomography inversion using the CRS attributes as the inputs.

The value of the wave filed attributes of the proposed method are mentioned for each round and compared with CRS wave filed attributes in Table 2 for a specific sample at CMP number 96 and 2.492 second. Given the value of the coherence for the proposed method, which started from 0.7595 at the first round and reaches to the 0.9418 at the fifth round compared to the one-step CRS coherence which is 0.4963, it can be concluded that the attributes of the proposed method are more reliable.

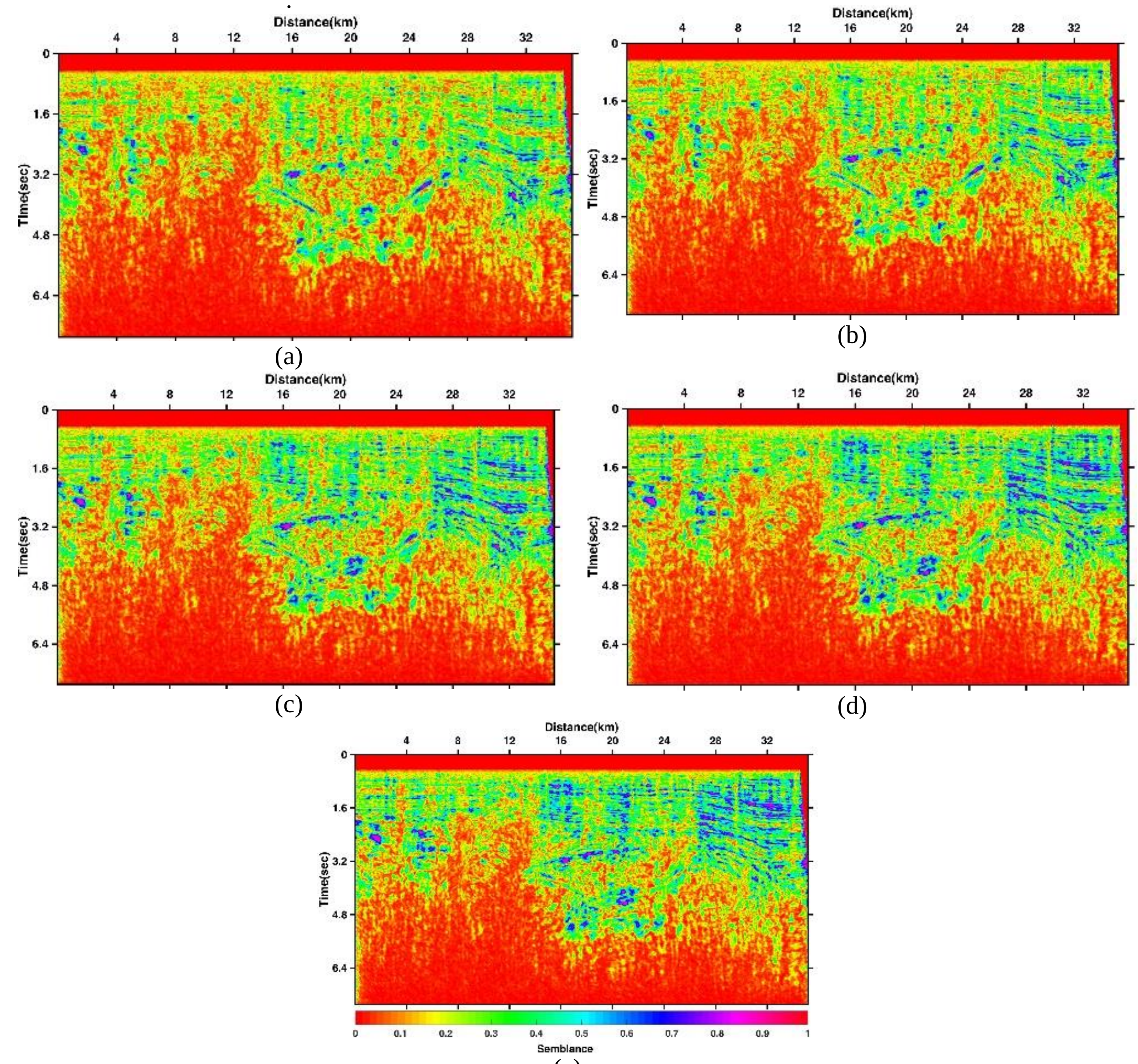

Figure 5: The coherence section in each round increased from ‘a’ to ‘e’, round one to five respectively.

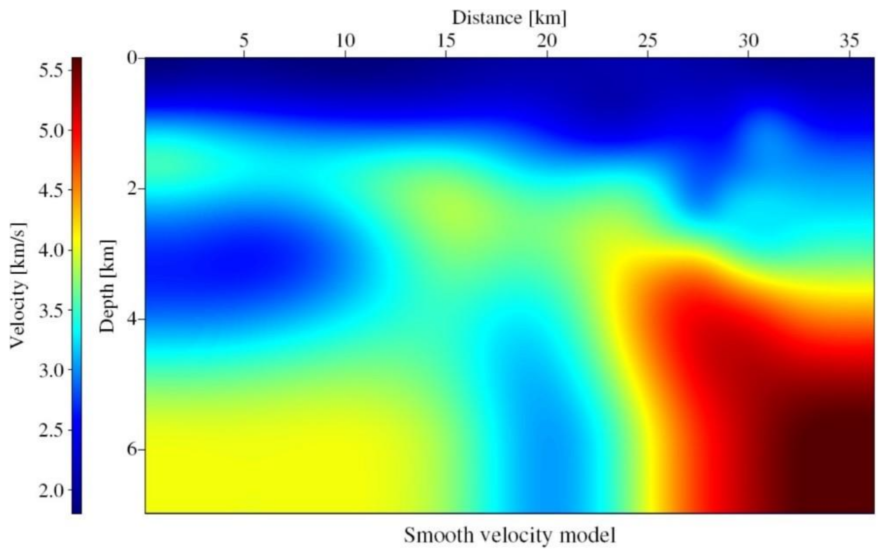

Figure 6: The smooth velocity obtained by CRS attributes as input to the NIP tomography inversion

Table 2. Comparison of the CRS and proposed method wave filed attribute for CMP number 96 and 2.492 second.

Method	Round	Attribute name	Value	Unit
CRS	1	Coherence	0.4963	-
	1	Rnip	6210.8	meter
	1	Angle	3.9444	degree
CDS	1	Coherence	0.7595	-
	1	Rnip	11392	meter
	1	Angle	4	degree
	2	Coherence	0.7980	-
	2	Rnip	9989.9	meter
	2	Angle	4	degree
	3	Coherence	0.9078	-
	3	Rnip	6774.9	meter
	3	Angle	4	degree
	4	Coherence	0.9399	-
	4	Rnip	5582	meter
	4	Angle	4	degree
	5	Coherence	0.9418	-
	5	Rnip	4982.5	meter
	5	Angle	4	degree

To validate the proposed method, the final smooth velocity models shown in Figure 4d and Figure 6 are applied for pre-stack depth migration. Figure 7 depicts the calculated CIG. These CIGs are obtained by performing the NIP tomography on the smooth velocity model and are calculated by the proposed method.

Figure 8 presents the CIG counterpart depicted in Figure 7. These CIGs are obtained using CRS attributes. However, in some CIG migrated by using the smooth velocity model obtained by the inversion of CRS attribute, shown in Figure 6, the CIG become flat.

Almost all events in the CIGs of Figure 7 are flat, confirming the accuracy of the velocity model. In comparison, in their counterpart CIG in Figure 8, the events are tilted, suggesting the inaccuracy of the velocity model.

4 Conclusions

The NIP wave tomography inversion uses the byproduct of the CRS stack method. Instead of R_{NIP}, which is calculated by CRS, we proposed using R_{CDS} generated by the model-based CDS stack method, which is not affected by R_N. The smooth velocity model is iteratively refined by model-based CDS stack method and NIP wave tomography inversion. In this study, after five iterations, the change in the velocity model was not significant. The coherence for a selected point for the proposed method increase from 0.7980 to 0.9418 while the coherence obtained by applying the CRS for the same point is 0.4963, which shows the more reliable attributes for the proposed method. Moreover, the event on the CIGs becomes flat after pre-stack depth migration, indicating the accuracy of the velocity model. In comparison, the events that are not flat when using smooth velocity were obtained by applying the CRS attributes.

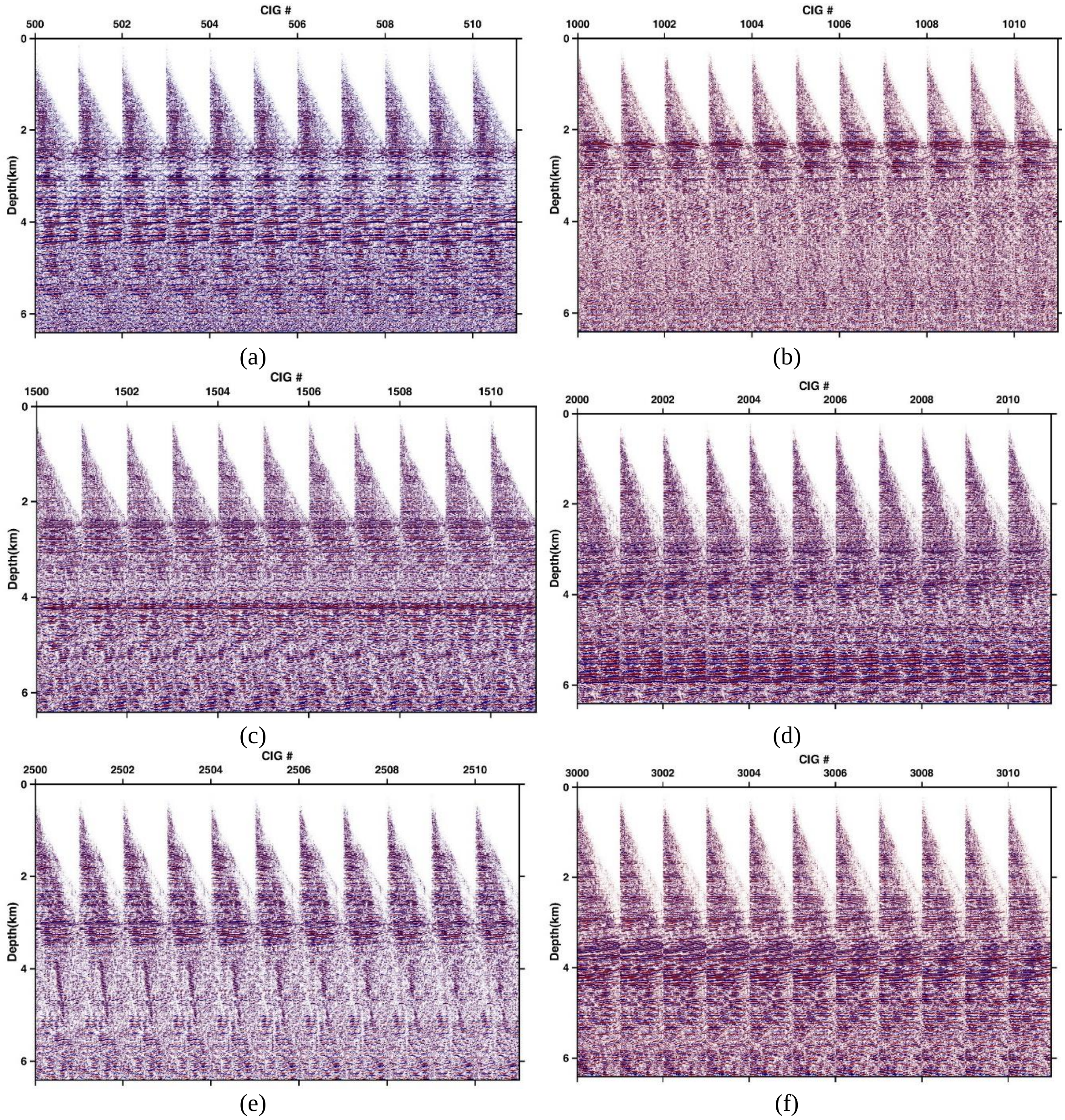

Figure 7: Pre-stack depth migration of the data with smooth velocity model obtained by proposed method, a) CIG from 500 to 510, b) CIG from 1000 to 1010, c) CIG from 1500 to 15010, d) CIG from 2000 to 2010, e) CIG from 2500 to 2510, and f) CIG from 3000 to 3010

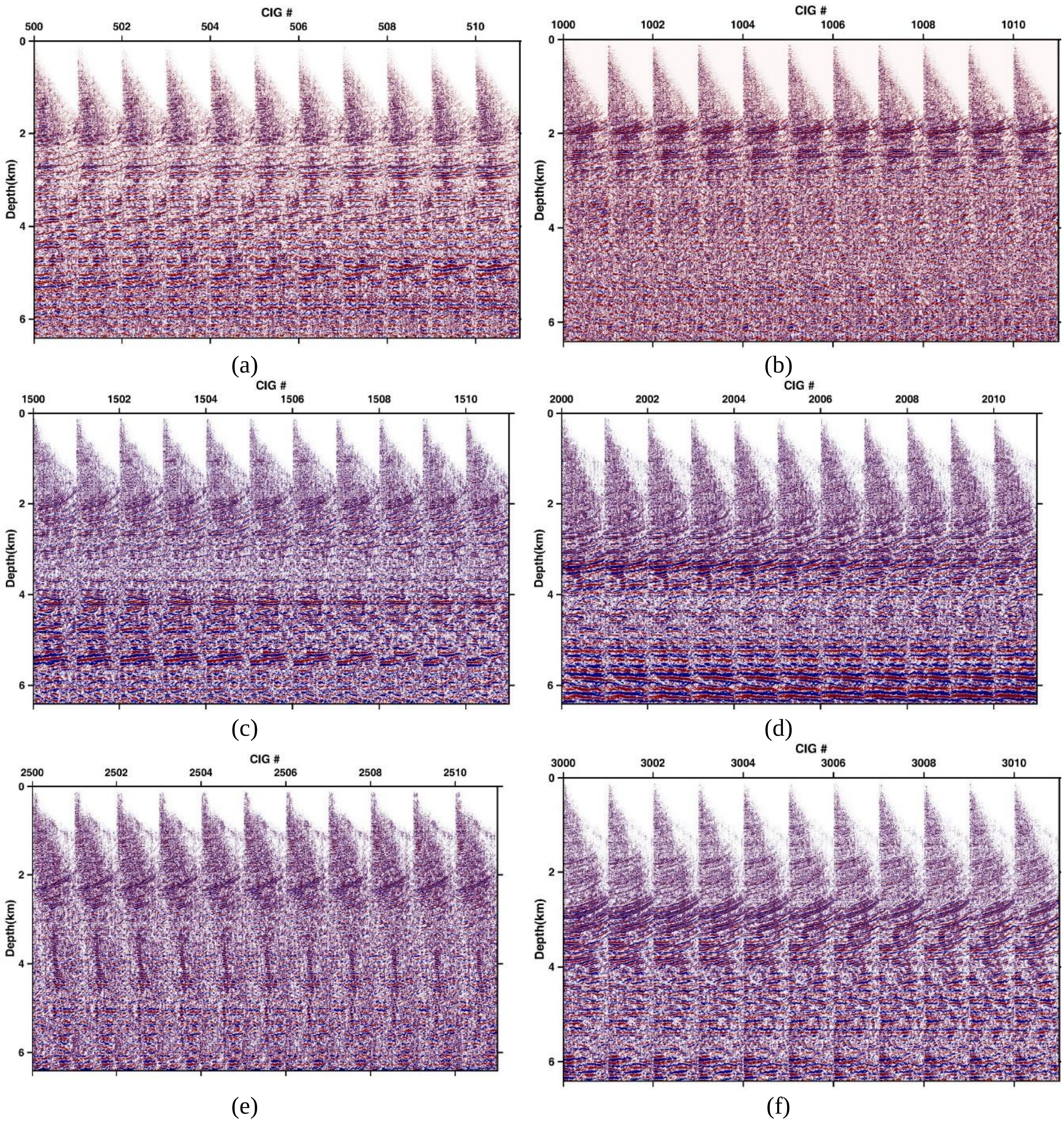

Figure 8: Pre-stack depth migration of the data with smooth velocity model obtained by CRS stack attributes, a) CIG from 500 to 510, b) CIG from 1000 to 1010, c) CIG from 1500 to 15010, d) CIG from 2000 to 2010, e) CIG from 2500 to 2510, and f) CIG from 3000 to 3010.

References

Baykulov, M., Gajewski, D., 2009, Prestack seismic data enhancement with partial common-reflection-surface (CRS) stack. Geophysics, 74, 49–58. https://doi.org/10.1190/1.3106182.

Duveneck, E., 2004, Velocity model estimation with data-derived wavefront attributes. Geophysics, 69, 265–274. https://doi.org/10.1190/1.1649394.

Duveneck, E., Hubral, P., 2002, Tomographic velocity model inversion using kinematic wavefield attributes, in: SEG Technical Program Expanded Abstracts 2002. Society of Exploration Geophysicists, pp. 862–865. https://doi.org/10.1190/1.1817398.

Hertweck, T., Schleicher, J., Mann, J., 2007, The Leading Edge. Lead. Edge 26, 818–827. https://doi.org/https://doi.org/10.1190/1.2756859.

Höcht, G., de Bazelaire, E., Majer, P., Hubral, P., 1999, Seismics and optics: Hyperbolae and curvatures. J. Appl. Geophys., 42, 261–281. https://doi.org/10.1016/S0926-9851(99)00040-3.

Hubral, P., 1983, Computing true amplitude reflections in a laterally inhomogeneous earth. Geophysics, 48, 1051–1062. https://doi.org/10.1190/1.1441528.

Jäger, R., 1999, The Common-Reflection-Surface stack theory and application. MSc. thesis, Karlsruhe Institute of Technology, Karlsruhe, Germany.

Mann, J., 2002, Extensions and applications of the Common-Reflection-Surface Stack Method. Logos Verlag, Berlin.

Mann, J., Jager, R., Muller, T., Hocht, G., 1999, Common-reflection-surface stack — a real data example. J. Appl. Geophys., 42, 301–318. https://doi.org/10.1016/S0926-9851(99)00042-7.

Müller, T., Jäger, R., Höcht, G., 1998, Common reflection surface stacking method — imaging with an unknown velocity model. 68th Annu. Mtg., Soc. Expl. Geophys. Expand. Abstr., pp. 1764–1767.

Pahlavanloo, A., Soleimani, M., Gallo, C., 2017, Improving seismic image in complex structures by new solving strategies in the CO-CRS and the CO-CDS methods. Iran. J. Geophys., 10, 42–56.

Schleicher, J., Tygel, M., Hubral, P., 1993, Parabolic and hyperbolic paraxial two-point traveltimes in 3D media. Geophys. Prospect., 41, 495–513. https://doi.org/10.1111/j.1365-2478.1993.tb00581.x.

Shahsavani, H., 2011, A model-based approach to the common-diffraction-surface stack. PhD thesis, Shahrood University of Technology, Shahrood, Iran.

Shahsavani, H., Mann, J., Piruz, I., Peter, H., 2011, A model-based approach to the Common-Diffraction- Surface Stack—theory andsynthetic case study. J. Seism. Explor., 20, 289–308.

Soleimani, M., Piruz, I., Mann, J., Peter, H., 2009a, Common-Reflection-Surface stack: accounting for conflicting dip situations by considering all possible dips. J. Seism. Explor., 18, 271–288.

Soleimani, M., Piruz, I., Mann, J., Peter, H., 2009b, Solving the Problem of Conflicting Dips in Common-Reflection-Surface (CRS) Stack. Ext. Abstr. 1st Internat. Conf. Exhib., Shiraz, Iran. Eur. Assn. Geosci. Eng.

Soleimani, M., Rafiei, M., 2016, Imaging seismic data in complex structures by introducing the partial diffraction surface stack method. Stud. Geophys. Geod., 60, 644–661, https://doi.org/10.1007/s11200-015-0942-6.

Tygel, M., Müller, T., Hubral, P., Schleicher, J., 1997, Eigenwave based multiparameter traveltime expansions. 67th Annu. Internat. Mtg., Soc. Expl. Geophys. Expand. Abstr., 1770–1773. https://doi.org/10.1190/1.1885776.